

Effects of electron dynamics in toroidal momentum transport driven by ion temperature gradient turbulence

I Holod and Z Lin

Department of Physics and Astronomy, University of California, Irvine, CA 92697, USA

E-mail: iholod@uci.edu

Received 20 October 2009, in final form 6 January 2010

Published 22 January 2010

Online at stacks.iop.org/PPCF/52/035002

Abstract

Several issues in the toroidal angular momentum transport by the ion temperature gradient (ITG) turbulence are addressed in this work: the system size effect in the momentum transport, the symmetry breaking mechanism for the generation of the spontaneous rotation and the effect of the trapped electron dynamics. We find that the magnitude of the momentum flux scales with the system size according to the gyroBohm scaling, with no significant size effect on the radial structure of the perturbed toroidal angular momentum. The symmetry breaking due to the shear of the radial electric field is found to be a mechanism for generating the residual momentum flux. However, it is small compared with the momentum pinch term in the case of a finite background rotation. The trapped electrons in the ITG turbulence increase the intensity and modify the spectral properties of the electrostatic fluctuations, leading to the increase in the toroidal momentum pinch.

(Some figures in this article are in colour only in the electronic version)

1. Introduction

Momentum transport is one of the topics of current interest in fusion research. Recent experimental and theoretical works [1–8] made significant progress toward the understanding of the momentum transport mechanisms. The radial flux of toroidal angular momentum can generally be decomposed into a diagonal (conductive) and off-diagonal (convective and residual stress) parts

$$\Gamma_{\phi} = -\chi_{\phi} \frac{d}{dr} \langle R^2 \omega_{\phi} \rangle + \Gamma_{\phi}^{\text{conv}} + S, \quad (1)$$

where ω_{ϕ} is the toroidal angular frequency, R is the tokamak major radius, χ_{ϕ} is the toroidal momentum conductivity, $\Gamma_{\phi}^{\text{conv}}$ is the convective flux of the toroidal momentum and S is the residual stress flux. The angular brackets mean flux-surface averaging.

The convective flux can be decomposed into a particle convection, i.e. the toroidal momentum carried by the particle flux, and the remaining part, which we would call rotation convective flux or toroidal momentum pinch flux

$$\Gamma_{\phi}^{\text{conv}} = \frac{1}{n} \Gamma_n \langle R^2 \omega_{\phi} \rangle + V_{\phi} \langle R^2 \omega_{\phi} \rangle. \quad (2)$$

The conductive flux is well understood and can usually be described by means of the quasilinear theory [7, 8]. The off-diagonal parts of the momentum flux, in particular the momentum pinch, are more complicated since there are several possible mechanisms responsible for the generation of the off-diagonal flux [3–5]; however, their relative importance has not been clearly established.

To gain a better understanding of the physics picture for the off-diagonal momentum transport, we run global gyrokinetic particle simulations of tokamak plasmas with zero and finite background rotation in the presence of drift wave turbulence. In our previous work [8], we have done simulations of toroidal angular momentum transport in the ion temperature gradient (ITG) turbulence with an adiabatic electron approximation using the gyrokinetic toroidal code GTC [10]. An off-diagonal momentum flux has been clearly observed in the case with rigid background rotation. Moreover, in the sheared rotation case, the conductive momentum flux has been observed and explained by means of a quasilinear theory. The intrinsic Prandtl number was measured in the simulation and also calculated analytically [8]. In this work we extend the previous studies to include kinetic trapped electrons in our gyrokinetic particle simulations of the momentum transport by the ITG turbulence. It has been shown earlier that the kinetic effects of the passing electrons have negligible contribution to the ITG turbulence [9]. Several aspects of momentum transport are studied in this paper. First, we consider the influence of the system size on the momentum transport. We have found that momentum flux increases with the size, consistent with the gyroBohm scaling. The characteristic scales of perturbed momentum structures remain the same in terms of the ion gyroradius. Next, we focus on the k_{\parallel} symmetry breaking due to the radial electric field shear, as a possible mechanism driving the off-diagonal flux [4]. We show that the E'_r profile, obtained as the turbulence-generated zonal flow shear, correlates with the mean k_{\parallel} profile and momentum flux profile in the case with zero background rotation. However, in the presence of a finite background rotation, other pinch generating mechanisms are dominant. Finally, the effects of kinetic electrons are studied for the cases of zero and finite rotation. Simulation results show that in the presence of trapped electrons the toroidal momentum pinch increases in proportion to the increase in the ion heat conductivity due to the modification of the turbulence intensity and the spectral structure by the trapped electrons.

2. Model description

In the GTC simulation, the perturbed distribution function of gyrocenter is solved using the nonlinear gyrokinetic equation. The equilibrium distribution function f_0 is chosen to be the local Maxwellian shifted with a parallel velocity

$$f_0 = \frac{n}{(2\pi T/m)^{3/2}} \exp \left[-\frac{2\mu B + m(v_{\parallel} - v_{\parallel 0})^2}{2T} \right]. \quad (3)$$

The background parallel rotation velocity is assumed to be small, $v_{\parallel 0} \ll v_i$ with slow spatial variation, such that the effect of rotation on the gyrokinetic equations [11] can be ignored. Representing the ion distribution function f as the sum of an equilibrium f_0 and a perturbed part δf , $f = f_0 + \delta f$ and taking into account the form of the equilibrium distribution

function (3), the electrostatic gyrokinetic equation for ion particle weight $w_i = \delta f_i / f_i$ can be written as

$$\frac{dw_i}{dt} = (1 - w_i) \left[-\boldsymbol{\kappa} \cdot \tilde{\mathbf{v}}_E - \frac{Z_i}{T_i} (v_{\parallel} - v_{\parallel 0}) \hat{\mathbf{b}} \cdot \nabla \delta \phi - \frac{1}{T_i} (\mu B + m_i (v_{\parallel}^2 - v_{\parallel} v_{\parallel 0})) \frac{\nabla B}{B} \cdot \tilde{\mathbf{v}}_E \right], \quad (4)$$

where T_i , m_i and Z_i are the ion temperature, mass and charge, respectively. The $E \times B$ drift velocity is $\mathbf{v}_E = \bar{\mathbf{v}}_E + \tilde{\mathbf{v}}_E$, $\bar{\mathbf{v}}_E = \frac{c}{B} \hat{\mathbf{b}} \times \nabla \phi_0$, $\tilde{\mathbf{v}}_E = \frac{c}{B} \hat{\mathbf{b}} \times \nabla \delta \phi$, with $\delta \phi$ being the perturbed electrostatic potential and

$$\boldsymbol{\kappa} = \frac{\nabla n_i}{n_i} + \left[\left(\frac{\mu B}{T_i} + \frac{m_i (v_{\parallel} - v_{\parallel 0})^2}{2T_i} \right) - \frac{3}{2} \right] \frac{\nabla T_i}{T_i} + \frac{m (v_{\parallel} - v_{\parallel 0}) \nabla v_{\parallel 0}}{T_i}$$

is the gradient of equilibrium density, temperature and toroidal velocity.

A fluid-kinetic hybrid model is used to describe the evolution of the electron distribution function [9, 12, 13]. The electron response is expanded using a smallness parameter $\delta = \omega / \omega_e \ll 1$, where ω is the mode frequency and ω_e is the electron transit frequency,

$$f_e = f_0 e^{e\delta\phi/T_e} + \delta h_e.$$

In the lowest order, the electron response is adiabatic,

$$\frac{\delta n_e}{n_0} = e^{e\delta\phi^{(0)}/T_e}.$$

At the higher order, the dynamics of electrons (in particular, the trapped electrons) is treated using the drift kinetic equation, modified by the presence of the background rotation

$$\begin{aligned} \frac{dw_e}{dt} = & \left(1 - \frac{e\delta\phi^{(0)}}{T_e} - w_e \right) \left[-\tilde{\mathbf{v}}_E \cdot \boldsymbol{\kappa} - \frac{\partial}{\partial t} \frac{e\delta\phi^{(0)}}{T_e} - \frac{m_e}{T_e} v_{\parallel 0} v_{\parallel} \frac{\nabla B}{B} \cdot \tilde{\mathbf{v}}_E \right. \\ & \left. + \left(-\frac{c}{eB} (\mu B + m (v_{\parallel}^2 - v_{\parallel 0} v_{\parallel})) \hat{\mathbf{b}} \times \frac{\nabla B}{B} + \tilde{\mathbf{v}}_E \right) \cdot \nabla \frac{e\langle\phi\rangle}{T_e} + \frac{e}{T_e} v_{\parallel 0} \hat{\mathbf{b}} \cdot \nabla \delta\phi^{(0)} \right], \end{aligned} \quad (5)$$

where $w_e = \delta h_e / f_e$.

The electrostatic potential is corrected at the higher order by the electron non-adiabatic response [9, 13].

3. Results and discussions

In our simulations, toroidal angular momentum transport is driven by the electrostatic collisionless ITG turbulence with the following parameters at a minor radius $r = 0.5a$: $R_0/L_T = 6.9$, $R_0/L_n = 2.2$, $a/R_0 = 0.358$, $a/\rho_i = 250$ or 500 and $T_e/T_i = 1$, where R_0 and a are the tokamak major (on the axis) and minor radii; L_T and L_n are the equilibrium temperature and density gradient scale lengths; T_e and T_i are the electron and ion temperatures, respectively, and ρ_i is the ion gyroradius. The safety factor is $q = 0.581 + 1.092r/a + 1.092(r/a)^2$.

The toroidal angular momentum flux is calculated as a flux-surface-averaged value $\Gamma_{\phi} = m_i \langle \int dv R v_{\parallel} \delta f_i \tilde{v}_{Er} \rangle$. The particle flux $\Gamma_n = \langle \int dv \delta f_i \tilde{v}_{Er} \rangle$ in the adiabatic electron case is non-zero due to the toroidicity effect (see the appendix for details), but practically negligible. The perturbed toroidal angular momentum and momentum flux are normalized by $m_i R_0 v_i$ and $m_i R_0 v_i^2$, respectively, where v_i is the ion thermal velocity.

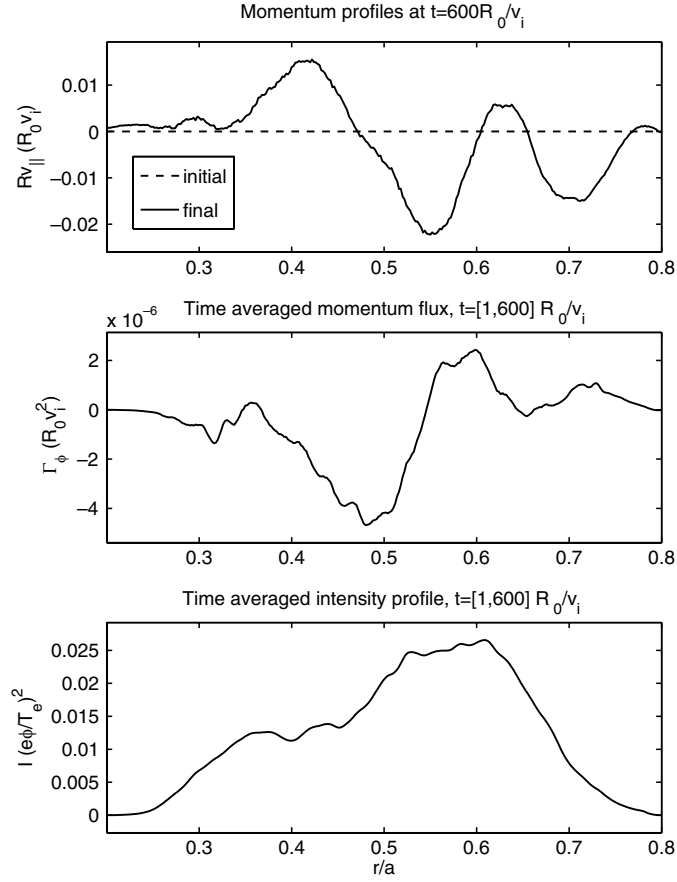


Figure 1. Radial profiles of toroidal angular momentum (upper panel), toroidal angular momentum flux (middle panel) and turbulence intensity (lower panel), for the case with adiabatic electrons, system size $a/\rho_i = 250$ and no background rotation.

We begin by considering the effect of the simulation system size for the ITG turbulence with adiabatic electrons. The perturbed momentum and momentum flux profiles obtained for the cases of $a/\rho_i = 250$ and $a/\rho_i = 500$ are shown in figures 1 and 2, respectively. As we can see, the radial structures of the perturbed momentum have approximately the same size in terms of ρ_i . The maximum perturbations of the toroidal momentum are larger in the case of smaller system size due to a stronger turbulence intensity, consistent with the gyroBohm scaling in the large device size regime (i.e. small $\rho^* = \rho_i/a$) [14] (lower panels of figures 1 and 2).

Next, the symmetry breaking and momentum flux generating mechanisms due to the radial electric field shearing [4] are examined. In figure 3 we compare the time-averaged profiles of the turbulence-generated zonal flow shear and the flux-surface-averaged parallel wavenumber defined as

$$\langle k_{||} \rangle = \frac{\int J d\theta d\zeta \frac{\sum_{\omega} k_{||} \delta\phi_{k_{||}\omega}^2}{\sum_{\omega} \delta\phi_{k_{||}\omega}^2}}{\int J d\theta d\zeta}$$

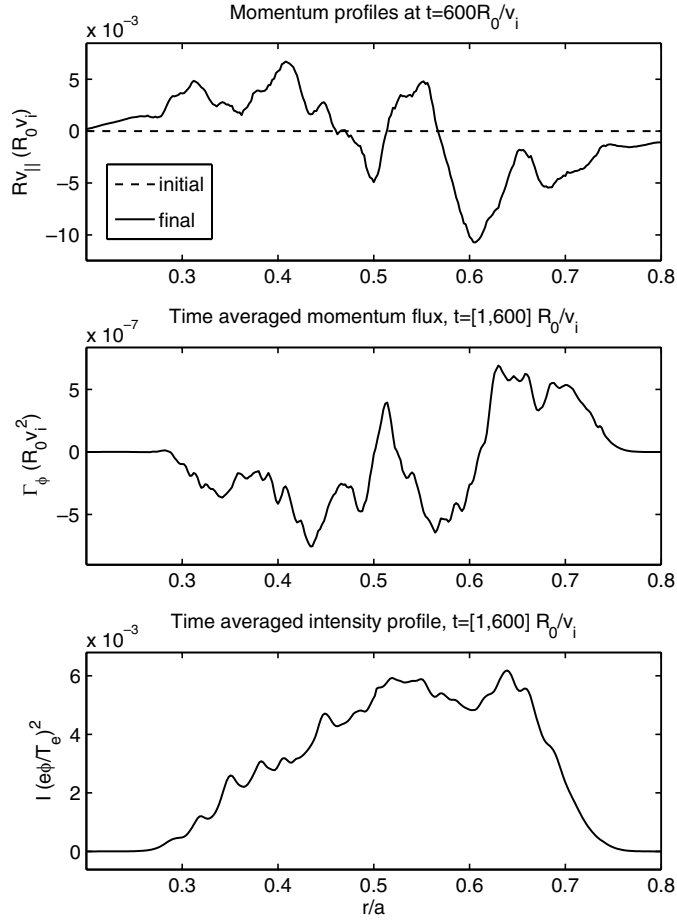


Figure 2. Radial profiles of toroidal angular momentum (upper panel), toroidal angular momentum flux (middle panel) and turbulence intensity (lower panel), for the case with adiabatic electrons, system size $a/\rho_i = 500$ and no background rotation.

where the Jacobian is [15]

$$J^{-1} \equiv \nabla\psi \cdot \nabla\theta \times \nabla\zeta = \frac{B^2}{gq + I}.$$

We have found rather strong correlation between these two profiles, with the correlation coefficient $C = 0.64$, calculated for two variables A and B as

$$C_{AB} = \frac{\sum_i (A_i - \bar{A})(B_i - \bar{B})}{\sqrt{\sum_i (A_i - \bar{A})^2 (B_i - \bar{B})^2}},$$

i.e. $C = 0$ indicating no correlation, $C = 1$ a perfect correlation and $C = -1$ anti-correlation.

In figure 4 we plot the radial profiles of $\langle k_{||} \rangle \langle \phi^2 \rangle$ and toroidal momentum flux. The correspondence between these profiles is characterized by the coefficient $C = 0.75$, which also indicates strong correlation. The flux-surface-averaged parallel wavenumber $\langle k_{||} \rangle$ is multiplied by the fluctuation intensity $\langle \phi^2 \rangle$ in order to match the proper radial envelope of the momentum flux. Note that the profile of fluctuation intensity is smooth (see lower

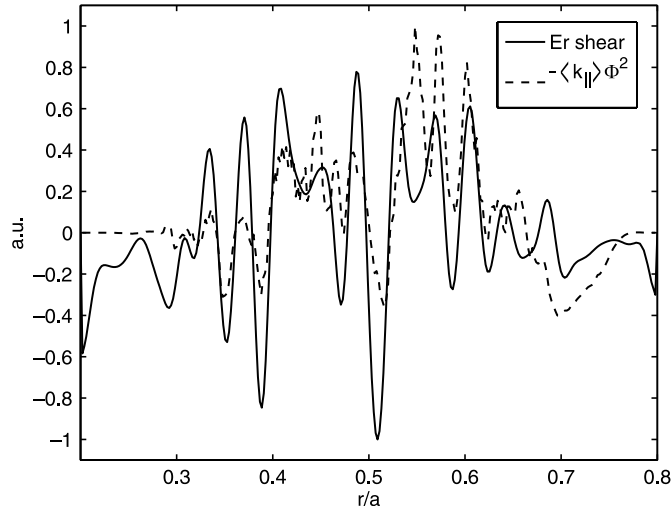


Figure 3. Time-averaged profiles of radial electric field shear and flux-surface averaged $\langle k_{\parallel} \rangle$, for the case with adiabatic electrons and no background rotation.

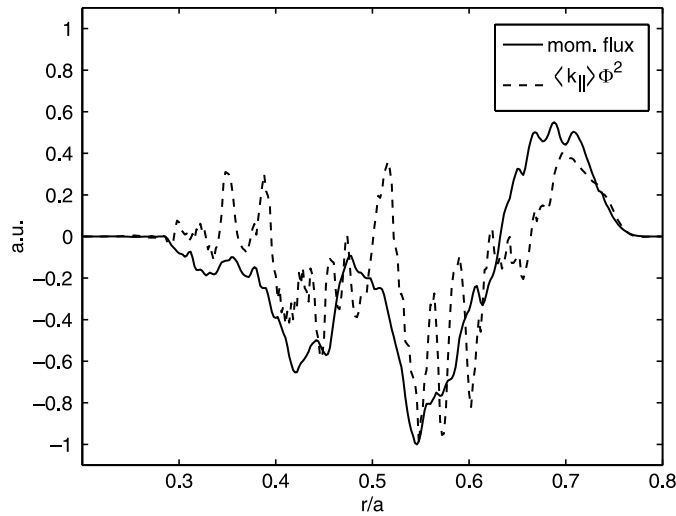


Figure 4. Time-averaged profiles of momentum flux and flux-surface averaged $\langle k_{\parallel} \rangle$, for the case with adiabatic electrons and no background rotation.

panels of figures 1 and 2) and itself cannot be responsible for the strong correlation between $\langle k_{\parallel} \rangle \langle \phi^2 \rangle$ and toroidal momentum flux. The results obtained so far confirm the role of the radial electric field shear in generating the residual stress component of the toroidal momentum flux.

However, in the case of a finite background rotation (figure 5), the $E \times B$ -shear and momentum flux profiles show no apparent correlation ($C = -0.05$), suggesting that the convective flux, which is stronger than the residual stress in this case, has a different driving mechanism [7]. As the evidence for pinch-like nature of the momentum flux in the rigid rotation cases, in figure 6 we plot the time evolution of the momentum flux for the cases

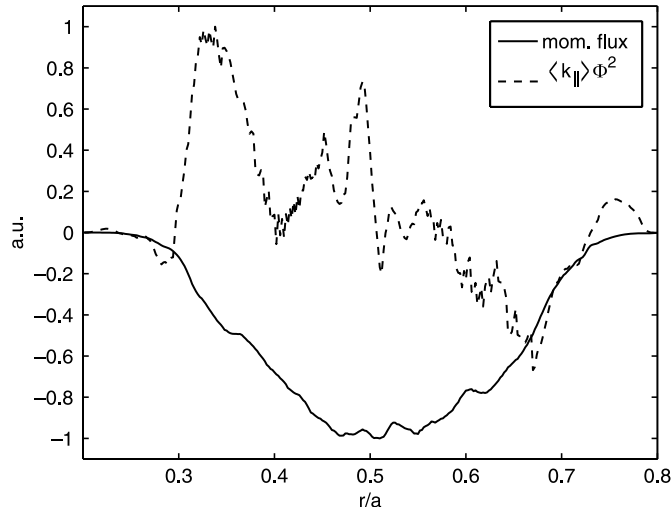


Figure 5. Time-averaged profiles of momentum flux and radial electric field shear, for the case with adiabatic electrons and rigid rotation at $\omega_{\phi} = 0.2v_i/R_0$.

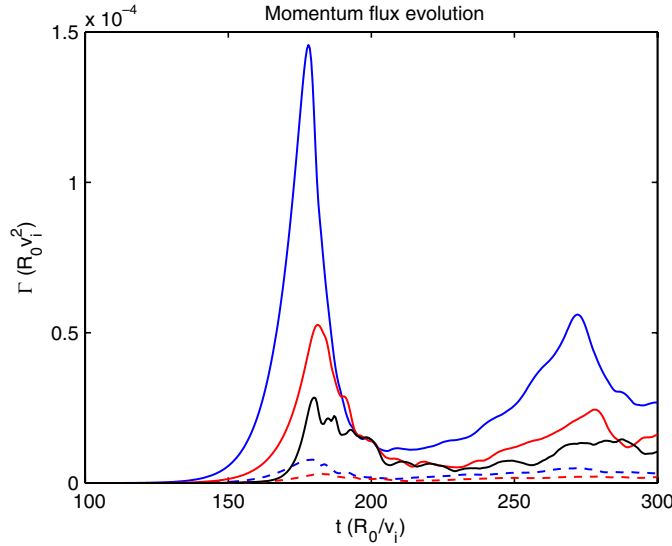


Figure 6. Time evolution of the rms value of total momentum flux (solid lines) and particle convective flux (dashed lines), for the case with kinetic electrons and rigid background rotation at $\omega_{\phi} = 0$ (black), $\omega_{\phi} = 0.1v_i/R_0$ (red) and $\omega_{\phi} = 0.2v_i/R_0$ (blue).

with kinetic electrons for different values of the background rotation velocity. As we can see, the momentum flux has a finite residual value at zero rotation and increases proportionally to the angular frequency ω_{ϕ} , indicating that it is consistent with the general form of equation (1).

We now focus on the effect of kinetic electrons on the momentum transport. To study the effect of kinetic electrons, we compare the radial profiles and time evolutions of the toroidal angular momentum and ion heat fluxes for the cases with adiabatic and kinetic electrons, respectively. In the top panel of figure 7, we plot the initial and perturbed profiles of the

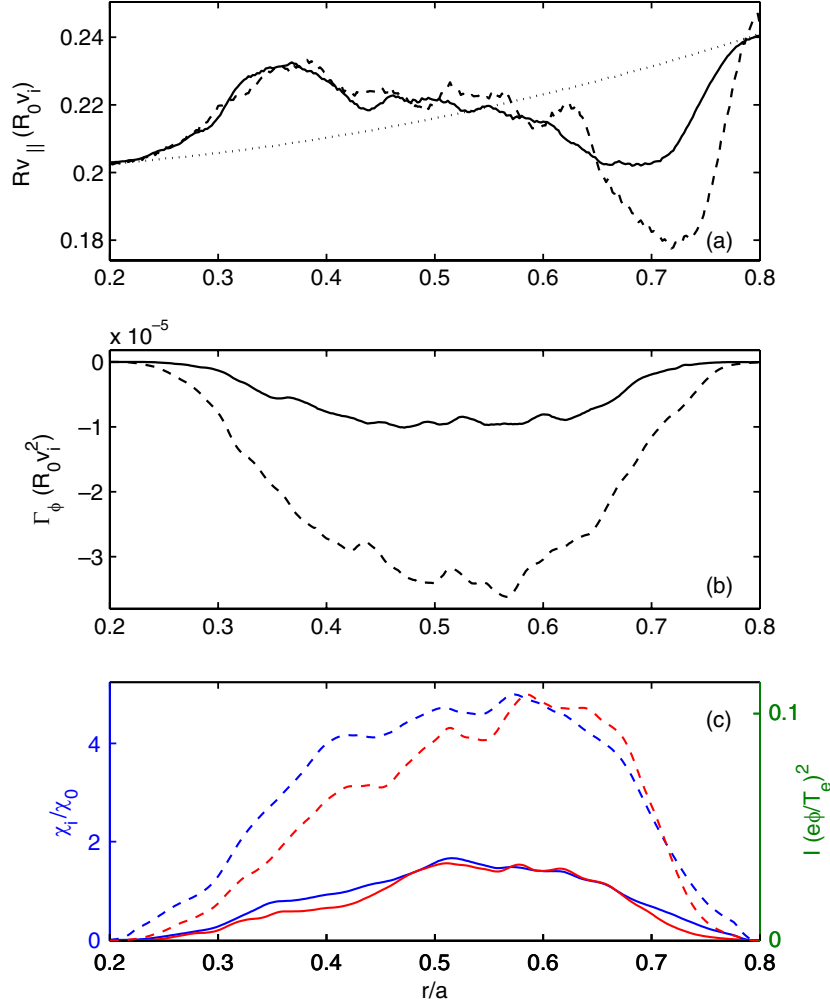


Figure 7. Initial (dotted line) and perturbed radial profiles of toroidal momentum (panel (a)), time-averaged toroidal momentum flux (panel (b)), time-averaged heat conductivity (blue line) and time-averaged turbulence intensity (red line) (panel (c)) for cases with adiabatic (solid line) and kinetic electrons (dashed line) with rigid rotation at $\omega_\phi = 0.2v_i/R_0$. Here, the turbulence intensity in the adiabatic electron case (red solid line in panel (c)) is multiplied by the factor of 1.5.

toroidal angular momentum for the case of rigid background rotation with an angular frequency of $\omega_\phi = 0.2v_i/R_0$. As we can see, in both the adiabatic and kinetic electron cases, there is a significant redistribution of the toroidal angular momentum, leading to the spinning up of a plasma toward the center of the tokamak.

In the middle panel of figure 7, we plot the radial profile of the momentum flux. Here, we observe the enhancement of the inward momentum flux in the kinetic electron case, similar to a theoretical result in [6].

Finally, in the bottom panel of figure 7, we plot the ion heat flux and turbulence intensity profiles. The correspondence between the two profiles in both the kinetic and adiabatic cases indicates that the ion heat transport is a diffusive process [16–18]. Here, we also observe the enhancement of both the ion heat flux and the turbulence intensity in the kinetic electron case [9, 19].

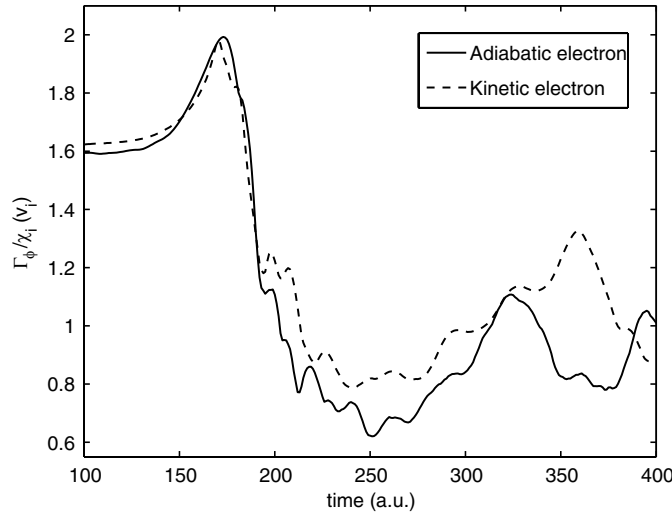


Figure 8. Time evolution of the rms value of momentum flux divided by the ion heat flux, for the case with rigid background rotation at $\omega_\phi = 0.2v_i/R_0$.

From the quasilinear theory we know that the momentum diffusivity is determined by the turbulence intensity and spectral properties of electrostatic fluctuations [8]. To separate these two factors, we divide the volume-averaged ion heat conductivity by the volume-averaged intensity. For the adiabatic electron case with a rigid rotation of $\omega_\phi = 0.2R_0/v_i$ this ratio is $(\chi_i/\chi_{GB})/(I/I_0) = 0.3$, where $\chi_{GB} = \rho^*cT_e/B$ and $I_0 = \rho^{*2}e^2/T_e^2$, while for the kinetic electron case the ratio is 0.2. These lead to the conclusion that kinetic electrons affect both turbulence intensity and spectral structure. The increase in the turbulence intensity when kinetic electrons are included is due to a reduction in the ITG mode dielectric constant by a reduction in the fraction of electrons that are adiabatic [9]. On the other hand, the ratio of the toroidal momentum flux to the ion heat conductivity remains roughly the same for both the adiabatic and the kinetic electron cases, as shown in figure 8. The fact that the ratio of the momentum pinch to the ion heat conductivity is independent of turbulent structure is similar to the theoretical results of [5, 20].

There is, as expected, a significant increase in particle convective flux in the case with kinetic trapped electrons, as shown in figure 9. However, this effect is unimportant, since the convective contribution to the total momentum flux is small in the ITG turbulence, with a typical value of about 10% (see figure 6 for example). However, it could be more important in the collisionless trapped electron turbulence where the particle flux could be much larger [21].

4. Conclusions

We have performed gyrokinetic simulation of the toroidal angular momentum transport in the presence of ITG turbulence. Cases with zero and finite constant background rotation are considered. Three aspects of momentum transport have been addressed: the effect of system size, the symmetry breaking mechanisms and the effect of kinetic electrons. We have found momentum flux increasing with the system size according to the gyroBohm scaling for large device size. The characteristic scales of perturbed momentum structures remain the same in terms of the ion gyroradius. We have observed a symmetry breaking due to the electric field

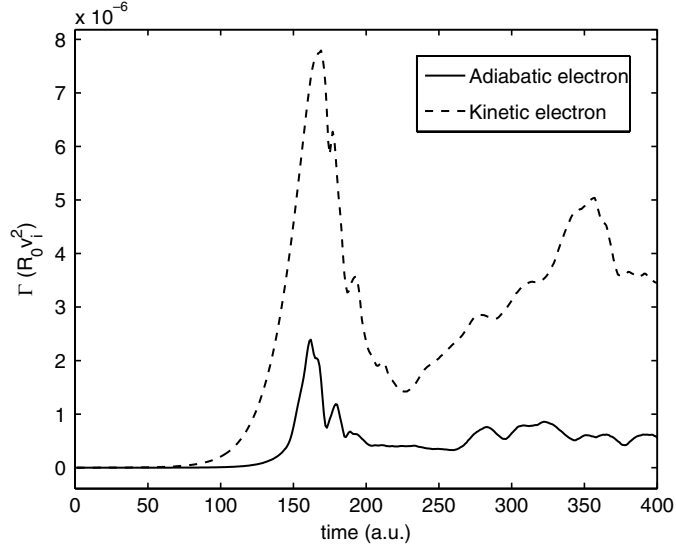


Figure 9. Time evolution of the rms value of convective momentum flux, for the case with rigid background rotation at $\omega_\phi = 0.2v_i/R_0$.

shear, correlating with a residual momentum flux. However, this correlation is subdominant in the presence of a finite background rotation. The effect of kinetic electrons has been investigated. Simulation results show that in the presence of trapped electrons the convective momentum flux increases by the same factor as the ion heat flux. This indicates that the physical mechanism for these enhancements is the same and it is related to the modification of the turbulent spectra and intensity by the kinetic electrons.

Acknowledgments

The authors gratefully acknowledge useful discussions with Y Xiao, W L Zhang, L Chen, P H Diamond and T S Hahm. Simulations have been performed using supercomputers at ORNL and NERSC. This work was supported by the US Department of Energy SciDAC GPS-TTBP, GSEP and Plasma Science centers.

Appendix. Particle flux in ITG turbulence with adiabatic electrons

The radial flux of particles in the ITG turbulence with adiabatic electrons can be expressed as

$$\Gamma_n = \langle \delta n_e \delta v_r \rangle \quad (6)$$

where the definition of the flux-surface averaging is

$$\langle \dots \rangle = \frac{\int_0^{2\pi} \int_0^{2\pi} \dots J \, d\theta \, d\zeta}{\int_0^{2\pi} \int_0^{2\pi} J \, d\theta \, d\zeta}. \quad (7)$$

The adiabatic electron response implies

$$\frac{\delta n_e}{n_0} = \frac{e\delta\phi}{T_e}. \quad (8)$$

We use Boozer coordinates (ψ, θ, ζ) , where ψ is the poloidal magnetic flux, θ is the poloidal angle, ζ is the toroidal angle and the Jacobian is [15]

$$J^{-1} \equiv \nabla\psi \cdot \nabla\theta \times \nabla\zeta = \frac{B^2}{gq + I}.$$

The covariant representation of the magnetic field in Boozer coordinates is

$$\mathbf{B} = I\nabla\theta + g\nabla\zeta + \delta\nabla\psi.$$

The perturbed velocity δv_r is the radial component of the perturbed $E \times B$ velocity

$$\delta v_r = \frac{\mathbf{B} \times \nabla\delta\phi}{B^2} \cdot \nabla\psi.$$

Decomposing the gradient as

$$\nabla\delta\phi = \frac{\partial\delta\phi}{\partial\theta}\nabla\theta + \frac{\partial\delta\phi}{\partial\zeta}\nabla\zeta + \frac{\partial\delta\phi}{\partial\psi}\nabla\psi,$$

we can write

$$\begin{aligned} \delta n_e \delta v_{Er} &= \frac{n_0 e \delta\phi}{T_e} \frac{\partial\delta\phi}{\partial\zeta} \frac{1}{B^2} I \nabla\theta \times \nabla\zeta \cdot \nabla\psi + \frac{n_0 e \delta\phi}{T_e} \frac{\partial\delta\phi}{\partial\theta} \frac{1}{B^2} g \nabla\zeta \times \nabla\theta \cdot \nabla\psi \\ &= \left(\delta\phi \frac{\partial\delta\phi}{\partial\zeta} I - \delta\phi \frac{\partial\delta\phi}{\partial\theta} g \right) \frac{n_0 e}{T_e} \frac{1}{gq + I}. \end{aligned} \quad (9)$$

For the circular cross-section tokamak $B = B_0 + B_1 \cos\theta$. Since $\delta\phi$ is periodic in the ζ and θ directions,

$$\int_0^{2\pi} d\zeta \delta\phi \frac{\partial\delta\phi}{\partial\zeta} = 0.$$

Let us represent $\delta\phi = \sum_m (\delta\phi_m^c \cos m\theta + \delta\phi_m^s \sin m\theta)$, then the following integral is non-zero only for the $m = 1$ harmonics, assuming $B_1 \ll B_0$

$$\int_0^{2\pi} d\theta \frac{1}{B^2} \delta\phi \frac{\partial\delta\phi}{\partial\theta} = \frac{3\pi B_1^2 \delta\phi_1^c \delta\phi_1^s}{2B_0^4}.$$

Thus, using equation (6), particle flux is

$$\Gamma_n = -\frac{3B_1^2 \delta\phi_1^c \delta\phi_1^s n_0 e g}{4B_0^4 T_e} \neq 0. \quad (10)$$

The divergence of the particle flux is also generally non-zero

$$\begin{aligned} \langle \nabla \cdot \Gamma_n \rangle &= \left\langle \frac{1}{J} \partial_\psi (J \Gamma_n \cdot \nabla\psi) \right\rangle \\ &= \frac{1}{4\pi^2} \int_0^{2\pi} \int_0^{2\pi} \frac{1}{J} \partial_\psi (J \Gamma_n \cdot \nabla\psi) J d\theta d\zeta = \partial_\psi \langle \Gamma_n \cdot \nabla\psi \rangle. \end{aligned}$$

This result can be generalized to the case of non-circular magnetic field configuration. In this case, the non-zero particle flux $\Gamma_n \propto \sum_{m=1}^{\infty} \phi_m^2 B_m^2$, where B_m is the poloidal harmonics of the equilibrium magnetic field. We note that the particle flux in equation (10) for the case of adiabatic electrons is much smaller than that for the case of kinetic electrons and is of the same order as some higher order terms neglected in the current formulation of the gyrokinetic theory.

References

- [1] Tala T *et al* 2009 *Phys. Rev. Lett.* **102** 075001
- [2] Yoshida M, Sakamoto Y, Takenaga H, Ide S, Oyama N, Kobayashi T and Kamada Y 2009 *Phys. Rev. Lett.* **103** 065003
- [3] Peeters A G, Angioni C and Strintzi D 2007 *Phys. Rev. Lett.* **98** 265003
- [4] Gurcan O D, Diamond P H, Hahm T S and Singh R 2007 *Phys. Plasmas* **14** 042306
- [5] Hahm T S, Diamond P H, Gurcan O D and Rewoldt G 2008 *Phys. Plasmas* **15** 055902
- [6] Peeters A G, Angioni C, Camenen Y, Casson F J, Hornsby W A, Snodin A P and Strintzi D 2009 *Phys. Plasmas* **16** 062311
- [7] Diamond P H, McDevitt C J, Gurcan O D, Hahm T S, Wang W X, Yoon E S, Holod I, Lin Z, Naulin V and Singh R 2009 *Nucl. Fusion* **49** 045002
- [8] Holod I and Lin Z 2008 *Phys. Plasmas* **15** 092302
- [9] Lin Z, Nishimura Y, Xiao Y, Holod I, Zhang W L and Chen L 2007 *Plasma Phys. Control. Fusion* **49** B163
- [10] Lin Z, Hahm T S, Lee W W, Tang W M and White R B 1998 *Science* **281** 1835
- [11] Hahm T S 1996 *Phys. Plasmas* **3** 4658
- [12] Nishimura Y, Lin Z and Chen L 2009 *Commun. Comput. Phys.* **5** 183
- [13] Holod I, Zhang W L, Xiao Y and Lin Z 2009 *Phys. Plasmas* **16** 122307
- [14] Lin Z and Hahm T S 2004 *Phys. Plasmas* **11** 1099
- [15] White R B and Chance M S 1984 *Phys. Fluids* **27** 2455
- [16] Holod I and Lin Z 2007 *Phys. Plasmas* **14** 032306
- [17] Lin Z, Holod I, Chen L, Diamond P H, Hahm T S and Ethier S 2007 *Phys. Rev. Lett.* **99** 265003
- [18] Zhang W L, Lin Z and Chen L 2008 *Phys. Rev. Lett.* **101** 095001
- [19] Chen Y, Parker S E, Cohen B I, Dimits A M, Nevins W M, Shumaker D, Decyk V K and Leboeuf J N 2003 *Phys. Plasmas* **43** 1121
- [20] Garbet X, Dubuit N, Asp E, Sarazin Y, Bourdelle C, Ghendrih P and Hoang G T 2005 *Phys. Plasmas* **12** 082511
- [21] Xiao Y and Lin Z 2009 *Phys. Rev. Lett.* **103** 085004